frontiers in Agronomy

TYPE Original Research
PUBLISHED 11 March 2026
DOI 10.3389/fagro.2026.1769313

OPEN ACCESS

EDITED BY
Ivan Vasenev,
Moscow Timiryazev Agricultural Academy, Russia

REVIEWED BY
Tamirat Solomon,
Wolaita Sodo University, Ethiopia
Raphael Beirigo,
Universidade Federal da Paraiba Fundacao de Apoio a Pesquisa e a Extensao, Brazil
José Luis Contreras Santos,
Colombian Corporation for Agricultural Research (AGROSAVIA), Colombia

*CORRESPONDENCE
Geomar Vallejos-Torres
gvallejos@unsm.edu.pe
Rodolfo Chuchon-Remon
rodolfo.chuchon@outlook.com

RECEIVED 16 December 2025
REVISED 01 February 2026
ACCEPTED 06 February 2026
PUBLISHED 11 March 2026

CITATION
Chuchon-Remon R, Solórzano R, Cruz J and Vallejos-Torres G (2026) Agroecosystems with greater canopy cover increase soil organic carbon density and reduce soil erodibility in the Peruvian Amazon.
Front. Agron. 8:1769313.
doi: 10.3389/fagro.2026.1769313

Agroecosystems with greater canopy cover increase soil organic carbon density and reduce soil erodibility in the Peruvian Amazon

Rodolfo Chuchon-Remon[1]*, Richard Solórzano[2], Juancarlos Cruz[2] and Geomar Vallejos-Torres[1,3]*

[1]Dirección de Servicios Estratégicos Agrarios, Instituto Nacional de Innovación Agraria (INIA), Estación Experimental Agraria El Porvenir, Juan Guerra, San Martín, Peru, [2]Dirección de Servicios Estratégicos Agrarios, Instituto Nacional de Innovación Agraria (INIA), Lima, Peru, [3]Facultad de Ciencias Agrarias, Universidad Nacional de San Martín, Tarapoto, San Martín, Peru

Introduction: Soil degradation in tropical agricultural landscapes represents one of the major challenges for sustainability and food security, particularly in the Peruvian Amazon. In this region, the loss of vegetative cover alters carbon storage and increases vulnerability to erosion. This study evaluated how gradients of canopy structure in representative agroecosystems—cassava with no canopy (CV-S), oil palm with intermediate canopy density (OP-S), cacao with medium-density canopy (CC-S), and coffee with high-density canopy (CF-S)—influence soil organic carbon density (SOCD) and erodibility (K factor).

Methods: A total of 1,049 soil samples (0–20 cm) were collected across three Amazonian regions and analyzed for their physical, chemical, and textural properties, complemented by multivariate and geostatistical analyses using ordinary kriging.

Results: Results showed that SOCD increased consistently with canopy density, from 32.68 t C ha^{-1} in CV-S to 82.64 t C ha^{-1} in CF-S. The Factor K exhibited the opposite pattern, decreasing from 0.31 to 0.16 as tree cover increased, indicating greater resistance to erosion. Erodibility was primarily determined by soil texture, with a strong positive correlation associated to silt content ($r = 0.89$) and a negative with sand content ($r = -0.74$). Likewise, SOCD showed a very high correlation with total nitrogen ($r = 0.96$), reflecting a tight coupling between carbon accumulation and nutrient availability under denser canopies. Principal component analysis further revealed that dense-canopy systems are related to higher SOCD and total nitrogen, whereas canopy-free systems are linked to higher bulk density and greater susceptibility to erosion.

Discussion: Spatial modeling showed that agroecosystems with more developed canopies exhibit better spatial structure and predictive performance, indicating a more stable edaphic organization under dense tree cover. Taken together, the results demonstrate that canopy structure functions as a key ecological regulator in Amazonian agroecosystems, with higher canopy cover promoting greater soil

carbon accumulation while reducing soil erodibility. This highlights that dense-canopy systems, such as coffee and cacao, represent effective strategies to strengthen the sustainability and resilience of agricultural landscapes in the Peruvian Amazon.

KEYWORDS

Amazonian agroecosystems, canopy structure, respect geostatistics, soil erodibility, soil organic carbon density, spatial variability

1 Introduction

Soil constitutes the functional backbone of agroecosystems, and its degradation represents one of the greatest challenges to global agricultural sustainability, particularly in the face of the growing demand for resilient and environmentally sound production systems (De Corato et al., 2024). In humid tropical regions such as the Amazon, this vulnerability is exacerbated by high rates of organic matter mineralization, the strong erosivity of rainfall, and agricultural practices that reduce vegetation cover—conditions that increase soil susceptibility to physical degradation and carbon loss (Rolo et al., 2023; Vallejos-Torres et al., 2023a). In this context, soil organic carbon density (SOCD) and soil erodibility (K factor) emerge as fundamental indicators for assessing soil resilience and the capacity of agricultural systems to sustain stable long-term production (Williams et al., 1984; Orton et al., 2014).

Numerous studies have shown that tree cover enhances soil fertility and physical stability by increasing litter inputs, enhancing soil organic carbon, and reducing aggregate breakdown (Zhu et al., 2020). Likewise, agroecosystems with shade trees have been shown to generate more favorable microclimatic conditions, enhance nutrient retention, and reduce erosion, although the magnitude of these effects strongly depends on canopy structure and crop type (Cerdá et al., 2020; Castellano-Hinojosa and Strauss, 2020). Despite the general consensus on the benefits of canopy cover in perennial systems, a critical knowledge gap remains: how variations in canopy density simultaneously influence soil organic carbon density (SOCD) and soil erodibility at the spatial scale in Amazonian agricultural landscapes.

In addition, vegetation cover reduces erosion intensity, significantly decreasing soil nutrient losses. These results illustrate the relationships between changes in vegetation cover, soil erosion, and nutrient export, which may provide a reference for conservation efforts and for improving soil quality (Zhao et al., 2020).

The Peruvian Amazon provides an ideal setting to evaluate these relationships due to its strong heterogeneity in agricultural practices and production systems, ranging from perennial crops such as coffee and cacao associated with shade trees to systems with lower canopy such as oil palm and cassava, characterized by greater soil exposure (Vallejos-Torres et al., 2023b). In this study, we evaluated how different canopy structures in representative agroecosystems of the Peruvian Amazon influence soil organic carbon density and soil erodibility by integrating physicochemical, statistical, and geostatistical analyses.

We hypothesized that agroecosystems with greater tree cover exhibit higher soil carbon stocks and lower erodibility due to increased biomass inputs, the action of roots and microorganisms, and enhanced stabilization of soil aggregates (Zeng et al., 2023; Gyssels et al., 2005). By addressing this knowledge gap, this research provides key quantitative evidence to support the design of soil management policies and sustainable agricultural practices in tropical regions of the Peruvian Amazon.

2 Materials and methods

2.1 Study of the site

The study was conducted in three departments of Peru: Loreto, San Martín, and Amazonas (Figure 1A). In the Loreto department, the study area was located in the province of Alto Amazonas, district of Yurimaguas, and corresponded to a cassava agroecosystem with no canopy cover (CV-S), covering an area of 46.93 km². In the San Martín department, the evaluated sites included the province of Tocache, district of Pólvora, representative of an oil palm agroecosystem with intermediate canopy cover (OP-S), encompassing an area of 122.93 km², as well as the province of Moyobamba, district of Soritor, corresponding to a cacao agroecosystem with medium-density canopy cover (CC-S), with a surface area of 154.46 km². In the Amazonas department, the study area was located in the province of Rodríguez de Mendoza and comprised a coffee agroecosystem characterized by high-density canopy cover (CF-S), covering an area of 86.81 km² (Figures 1B, C). The study was carried out between August and December 2024.

The San Martín region exhibits a tropical–subtropical climate with marked seasonality, mean annual temperatures ranging from 23 to 27 °C, and annual precipitation close to 1,500 mm (SENAMHI, 2014). In contrast, Loreto is entirely located within the humid Amazonian lowland and is characterized by an equatorial climate without a dry season, mean annual temperatures of 26–28 °C, and annual precipitation exceeding 2,500–3,000 mm. Meanwhile, Amazonas spans a gradient from lowland rainforest to the eastern slope of the Andean mountain range, exhibiting temperate–humid climates with temperatures ranging from 18 to 24 °C and annual precipitation between 1,500 and 2,500 mm (SERNANP, 2017).

The evaluated agroecosystems are distributed along an altitudinal gradient that conditions soil formation and the dominant edaphic processes. The canopy-free system CV-S, located in the low Amazonian plain (130–270 m a.s.l.), is mainly

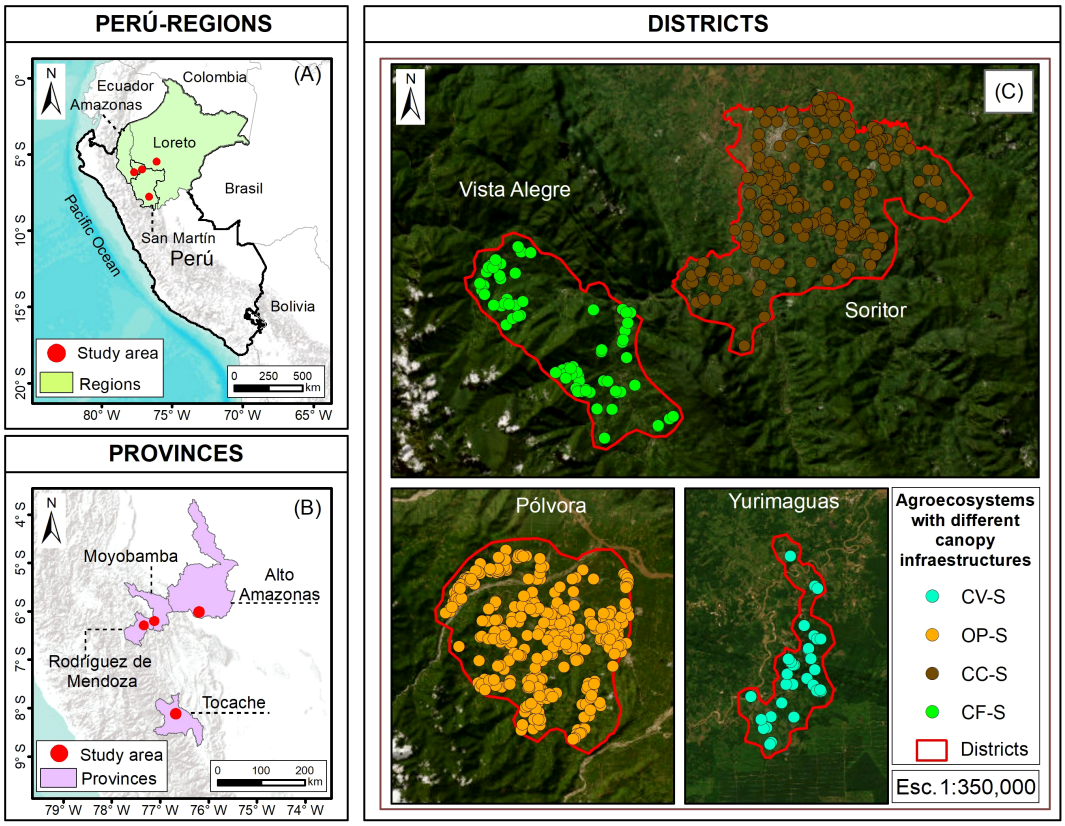

FIGURE 1
Location of the study areas in the Peruvian Amazon. **(A)** Evaluated regions: Amazonas, Loreto, and San Martín. **(B)** Provinces: Rodríguez de Mendoza, Moyobamba, Tocache, and Alto Amazonas. **(C)** Corresponding districts—Vista Alegre, Soritor, Pólvora, and Yurimaguas—and distribution of the sampling points associated with the four agroecosystems: cassava without canopy (CV-S), oil palm with intermediate canopy (OP-S), cacao with medium-density canopy (CC-S), and coffee with high-density canopy (CF-S).

associated with Dystric Cambisols and Haplic Acrisols (CMd–ACh) (Figures 2A1, B1). The OP-S system, developed across intermediate altitudinal ranges (450–900 m a.s.l.), exhibits greater edaphic heterogeneity, dominated by Eutric Leptosols, Eutric Cambisols, and Eutric Regosols (LPe–CMe–RGe) (Figures 2A2, B2). In contrast, agroecosystems with greater tree cover, CC-S and CF-S, located in colline and montane environments (800–2,200 m a.s.l.), are predominantly characterized by Eutric Regosols and Eutric Cambisols (RGe–CMe), as shown in Figures 2A3–B3, A4–B4, respectively. Soil classes were interpreted according to the FAO/WRB classification adopted by the National Institute of Natural Resources of Peru (INRENA, 1996), whereas altitudinal ranges were characterized using the Copernicus GLO-30 digital elevation model (European Space Agency [ESA], 2021).

2.2 Sampling design

Four agricultural agroecosystems were identified across four study zones: oil palm and cacao in the San Martín region, coffee in the Amazonas region, and cassava in Loreto. The oil palm agroecosystem with intermediate canopy cover (OP-S) consisted of plantations older than 15 years and included a ground cover dominated by *Pueraria phaseoloides* (Kudzu). Subsequently, 334 soil samples were collected in this agroecosystem. The cacao agroecosystem with medium-density canopy cover (CC-S) had plantation ages ranging from 8 to 10 years and was associated with shade trees, mainly *Cedrela odorata*, *Inga* sp., *Citrus sinensis*, *Musa* sp., among others; 601 soil samples were sampled for this system. The coffee agroecosystem (CF-S), characterized by high-density canopy cover and plantation ages between 9 and 12 years, was associated primarily with *Cedrela odorata*, *Inga* sp., *Calycophyllum spruceanum*, and *Schizolobium amazonicum*, among other species. From this agroecosystem, 71 soil samples were collected. Finally, the cassava agroecosystem without canopy cover (CV-S) or ground cover, established as a mono-agroecosystem, yielded 43 soil samples (Table 1). In total, 1,049 soil samples were collected at a depth of 0–20 cm using soil pits. This sampling depth was selected since soil organic carbon density (SOCD) is predominantly retained in the surface soil layer (~20 cm) and decreases with increasing soil depth (Hao et al., 2015).

2.3 Calculation of soil edaphic and nutritional parameters

The collected soil samples were analyzed at the accredited laboratory of the National Institute of Agrarian Innovation (INIA), Peru. Soil texture was determined using the hydrometer method. Soil pH was measured with a potentiometer in a 1:2.5 soil–water suspension. Soil organic matter (SOM) was determined following the NOM-021-RECNAT-2000 (2002). Total nitrogen was analyzed using the Kjeldahl method (Bremner, 1996), available phosphorus by the Olsen method (Olsen and Sommers,

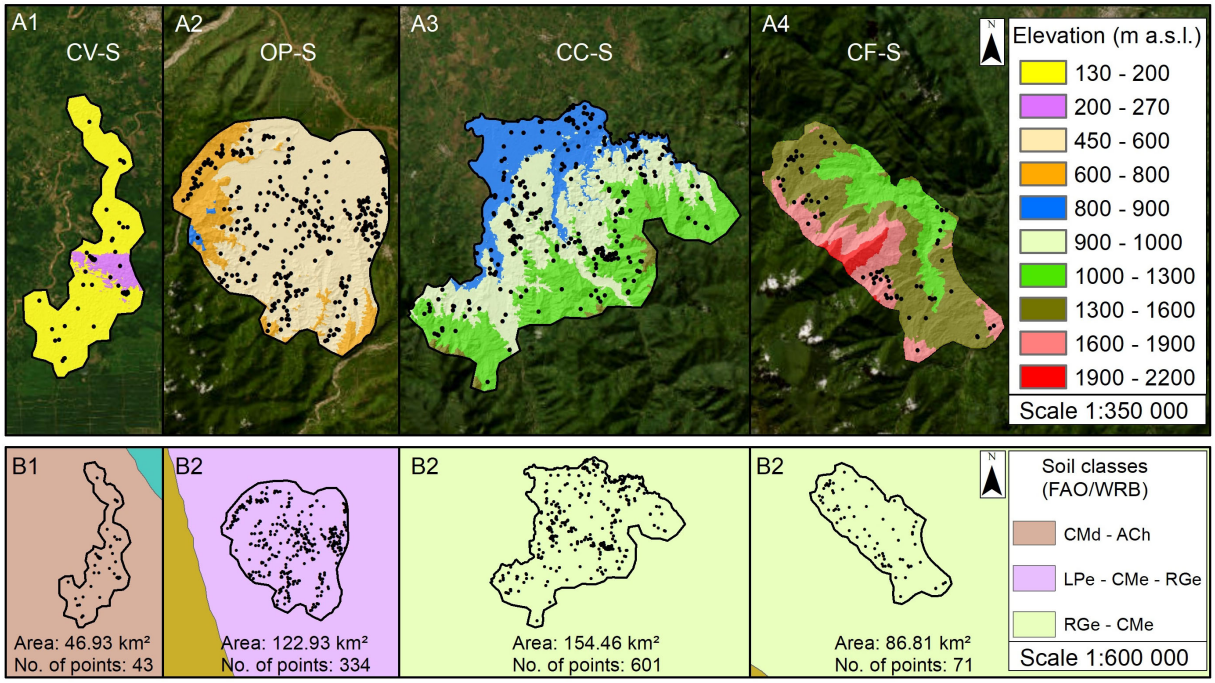

FIGURE 2
Spatial distribution of elevation and soil classes across the evaluated agroecosystems. (**A1–A4**) show the altitudinal ranges (m a.s.l.) for the cassava system without canopy cover (CV-S), oil palm with intermediate canopy cover (OP-S), cacao with medium-density canopy cover (CC-S), and coffee with high-density canopy cover (CF-S), respectively. (**B1–B4**) display the dominant soil class associations interpreted for the same agroecosystems: CMd–ACh, Dystric Cambisols–Haplic Acrisols LPe–CMe–RGe, Eutric Leptosols–Eutric Cambisols–Eutric Regosols and Eutric RGe–CMe, Regosols–Eutric Cambisols. Black dots indicate soil sampling locations.

1982), and available potassium according to the NOMA-021-RECNAT-2000 standard (2002).

2.4 Calculation of soil organic carbon density

Soil organic carbon stock (SOCD) represents the amount of organic carbon stored in the soil per unit area down to a given depth. SOCD was calculated following the mass-balance approach proposed by Batjes (1996) and was expressed in t C ha^{-1}, according to Equation 1:

$$SOCD = \rho \times P \times D \times (1 - S) \quad (1)$$

where ρ is soil bulk density (g cm^{-3}), P is soil organic carbon content (%), D is soil layer thickness, and S is the volumetric fraction of coarse fragments (> 2 mm).

2.5 Calculation of soil erodibility

Soil erodibility (K) is a fundamental parameter that quantifies the intrinsic resistance of soil to erosion as a function of its physical

TABLE 1 **Characteristics of the agroecosystems.**

Agroecosystem	Crop age and prior land use	Fertilization	Logging, burning, and tillage	Under the shade of tree species
Oil palm tree (*Elaeis guineensis*)	Coffee stands are 8–15 years old. Before crop establishment, the areas were covered with shrub vegetation.	Application of inorganic and organic fertilizers, generally potassium, dolomite, rock phosphate, and compost.	Logging was carried out, but no burning, for crop establishment. Weed control was performed manually (cultural control).	*Pueraria* sp
Cacao (*Theobroma cacao*)	Age greater than 8–10 years. Before crop establishment, the area was covered with fallow (purma) and forest.	With applications of island guano and compost.	No burning was carried out; only slashing and felling of vegetation.	Associated with trees of *Cedrela odorata*, *Inga* spp., *Guazuma crinita*, and *Cordia* sp. *Citrus sinensis*
Coffee (*Coffea arabica*)	Coffee stands are divided into ages of 7–12 years. Before crop establishment, the areas were covered with shrub vegetation.	Application of compost twice a year.	Logging was carried out, but no burning, for crop establishment.	Associated with trees of *Inga* spp., *Persea americana*, *Cedrela odorata* and *Calycophyllum* spruceanum.
Yuca (*Manihot esculenta*)	Annual crop. Before crop establishment, the areas were covered with shrub vegetation.	Without any fertilizer application	No burning was carried out; only slashing and felling of vegetation.	Weeds such as: *Portulaca oleracea*, *Setaria* sp, *Cyperus rotundus*, *Bidens* sp.

properties and organic carbon content. In this study, the K factor was estimated using the empirical formulation proposed by Williams et al. (1984). The calculation of the K factor was performed according to Equation 2:

$$K = [0.2 + 0.3\ e^{-0.0256\ SAN(1\ -\ \frac{SIL}{100})}]\left(\frac{SIL}{CLA\ +\ SIL}\right)^{0.3} \quad (2)$$

$$\left(1.0 - \frac{0.25\ C}{C + e^{(3.72\ -\ 2.95\ C)}}\right)\left(1.0 - \frac{0.7SN_1}{SN_1 + e^{(-5.51\ +\ 22.9\ SN1)}}\right)$$

donde SAN, SIL, CLA y C son los contenidos de arena, limo, arcilla y carbono orgánico del suelo (%), y $SN_1 = 1 - SAN/100$. Equation 2 allows K to vary approximately between 0.1 and 0.5. The first term provides low K values for soils with high contents of coarse sand; the second term reduces K values for soils exhibiting high clay-to-silt ratios; the third term reduces K values for soils with high organic carbon contents; and the fourth term further reduces K for soils with extremely high sand contents (SAN > 70%).

2.6 Statistical and geostatistical analyses

Boxplots were used to explore the distribution and variability of the data. A one-way analysis of variance (ANOVA) was applied to determine significant differences among group means classified according to land use in agroecosystems with different canopy structures, based on their physicochemical and textural soil properties. Prior to ANOVA, the assumptions of normality and homogeneity of variances were verified using the Shapiro–Wilk and Bartlett tests, respectively. When significant differences were detected ($p < 0.05$), Tukey's honestly significant difference (HSD) test was applied to identify distinct groups using grouping letters. Bivariate relationships among soil variables were explored using Pearson correlation analysis, allowing the identification of direct and inverse associations between soil organic carbon density (SOCD), the soil erodibility factor (K), and the physicochemical soil properties. In addition, a principal component analysis (PCA) was performed to synthesize the multivariate variability across the set of soil properties and to visualize clustering patterns associated with each agroecosystem. All statistical analyses were conducted using R (version 4.5.0; R Core Team, 2025) through the RStudio development environment (version 2025.05.0 + 496; Posit Team, 2025). Figures 3, 4, and 5, corresponding to *post hoc* mean comparison tests (Tukey HSD), were generated applying the agricolae, ggplot2, dplyr, readxl, and patchwork packages for data manipulation, analysis, and visualization. Figure 6, representing the USDA soil textural triangle, was created using the soiltexture package. Figure 7, showing the correlation matrix, was obtained through the Hmisc, ggplot2, and reshape2 packages. Finally, Figure 8, corresponding to the principal component analysis (PCA), was produced by means of FactoMineR, factoextra, and ggnewscale. This enables the generation of clear, reproducible, and high-quality scientific visualizations.

Geostatistical analysis was performed using the SmartMap plugin of QGIS version 3.34.14 (Prizren), applying the ordinary kriging method (QGIS Development Team, 2024; Pereira and Valente, 2022). This method allows modeling the spatial continuity of soil properties based on the dependence structure among point observations (Coulibaly, 2024). The process began with the construction of the experimental semivariogram from the sampled data, followed by the fitting of the theoretical model (spherical, exponential, or Gaussian) that best represented spatial variability. From this model, the nugget (C_0), sill ($C_0 + C_1$), and range (a) parameters were estimated, describing the magnitude and spatial extent of autocorrelation of the variable. Subsequently, ordinary kriging was applied to generate continuous maps of predicted values and associated estimation errors, ensuring accurate and consistent cartographic representation. Cross-validation was used to evaluate model performance through RMSE and R^2, indicators, thereby ensuring the reliability and consistency of the spatial predictions (Zarychta, 2025).

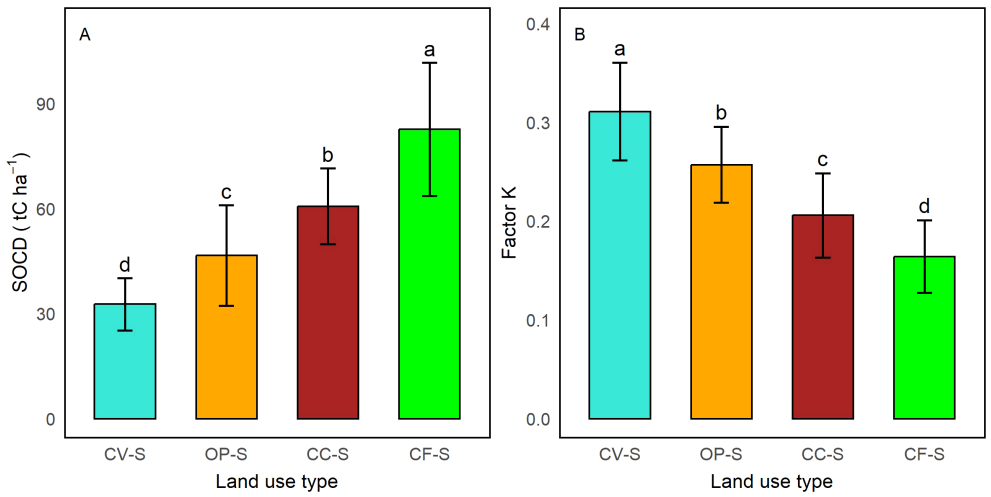

FIGURE 3
Comparison of four types of canopy structures: CV-S, OP-S, CC-S, and CF-S. **(A)** Soil organic carbon density (SOCD) increases from CV-S to CF-S. **(B)** Soil erodibility (Factor K) decreases from CV-S to CF-S. The bars indicate the mean ± standard deviation; letter annotations denote statistically significant differences according to Tukey's test ($p < 0.05$).

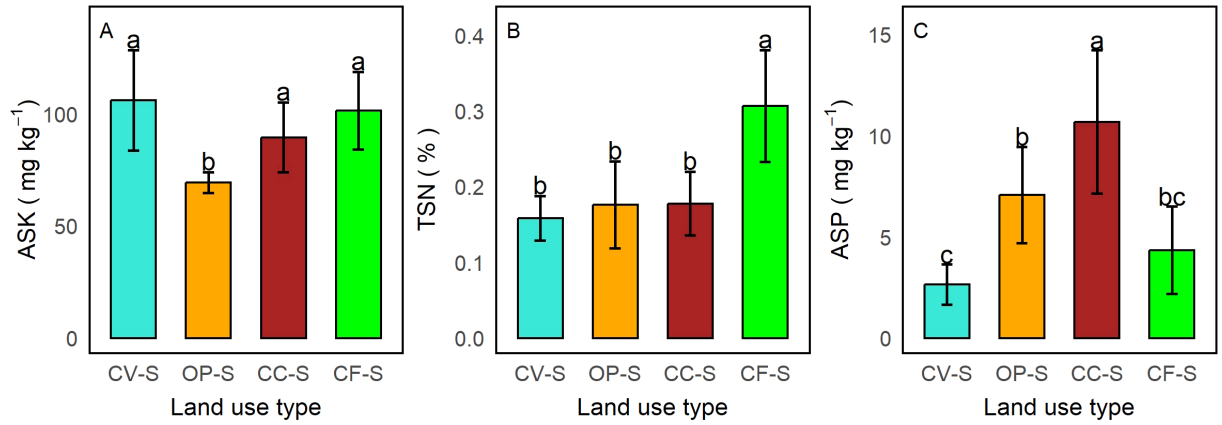

FIGURE 4
Comparison of four types of canopy structures: CV-S, OP-S, CC-S, and CF-S. **(A)** available soil potassium (ASK), **(B)** total soil nitrogen (TSN), and **(C)** available soil phosphorus (ASP). The bars indicate the mean ± standard deviation; letter annotations denote statistically significant differences according to Tukey's test ($p < 0.05$).

3 Results

3.1 Soil organic carbon density and the soil erodibility factor

Analysis of variance and Tukey's test ($p< 0.05$) revealed significant differences in soil organic carbon density (SOCD) and the soil erodibility factor (K) among land-use systems with different canopy structures (Table 2; Figures 3A, B, respectively). SOCD showed a progressive increase from the system without canopy (CV-S: 32.68 ± 7.51 t C ha^{-1}) to the high- density canopy system (CF-S: 82.64 ± 19.04 t C ha^{-1}), following the order CV-S< OP-S (46.59 ± 14.38 t C ha^{-1})< CC-S (60.66 ± 10.85 t C ha^{-1})< CF-S. The aforementioned indicates greater organic carbon accumulation

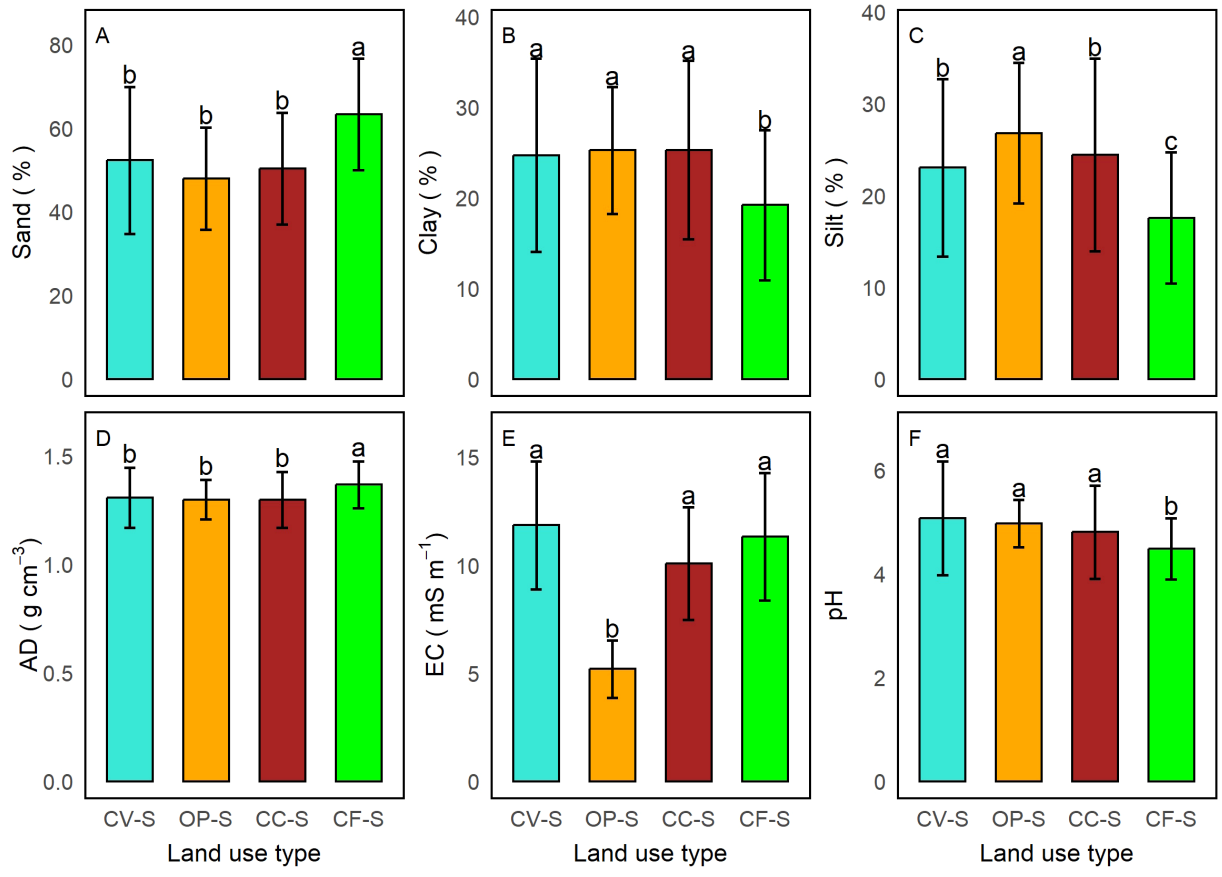

FIGURE 5
Comparison of four canopy structure types: CV-S, OP-S, CC-S, and CF-S. **(A)** sand content, **(B)** clay content, **(C)** silt content, **(D)** bulk density (BD), **(E)** electrical conductivity (EC), and **(F)** hydrogen potential (pH). Bars indicate the mean ± standard deviation; letter annotations denote statistically significant differences according to Tukey's test ($p < 0.05$).

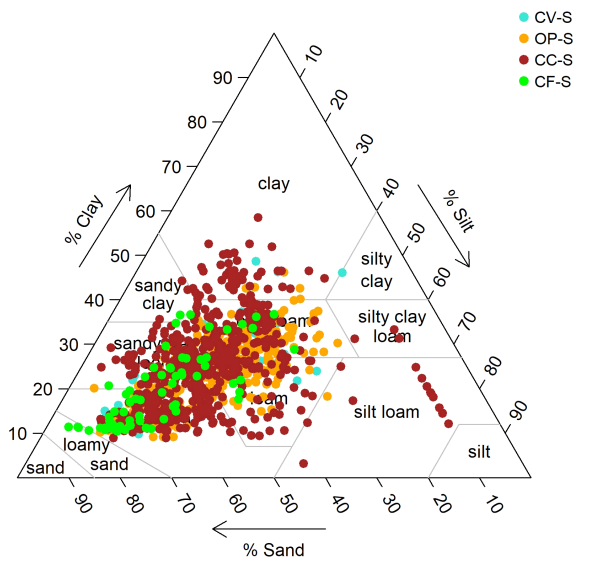

FIGURE 6
Soil texture triangle showing the distribution of samples across the different textural classes (USDA soil classification system).

under denser tree cover (Figure 3A). In contrast, the K factor exhibited an inverse pattern, with the gradient CF-S (0.16 ± 0.04)< CC-S (0.21 ± 0.04)< OP-S (0.26 ± 0.04)< CV-S (0.31 ± 0.05) (Figure 3B). This reflects a reduction in soil erodibility associated with increasing canopy cover and higher soil organic carbon content. These patterns may be partly associated with higher total soil nitrogen (TSN) and organic matter (OM) contents in soils of the CF-S system, as well as with differences in soil texture—particularly silt content—among land-use systems with contrasting canopy structures.

3.2 Soil nutrients under different canopy structures

The analysis of variance, complemented by Tukey's test ($p< 0.05$), revealed significant differences in several nutrients and physicochemical soil properties among systems with different associated canopy structures (Figure 4, Table 2). Soil nutrients such as available soil potassium (ASK) reached the highest values in the high density canopy system (CF-S: 104.8 ± 25.3 mg kg^{-1}) and in the non-canopy system (CV-S: 106.1 ± 23.9 mg kg^{-1}), with no significant differences between them, whereas the intermediate canopy system (OP-S: 69.2 ± 4.6 mg kg^{-1}) exhibited the lowest value (Figure 4A). Regarding total soil nitrogen TSN, the high density canopy system (CF-S) showed a significantly higher content (0.31 ± 0.07%) compared with the medium density canopy (CC-S: 0.18 ± 0.04%), intermediate canopy (OP-S: 0.18 ± 0.06%) and non-canopy systems (CV-S: 0.16 ± 0.03%) (Figure 4B). Total soil nitrogen (TSN) was generally affected by the organic matter (OM) content present in the CF-S system. In contrast, available soil phosphorus ASP displayed a

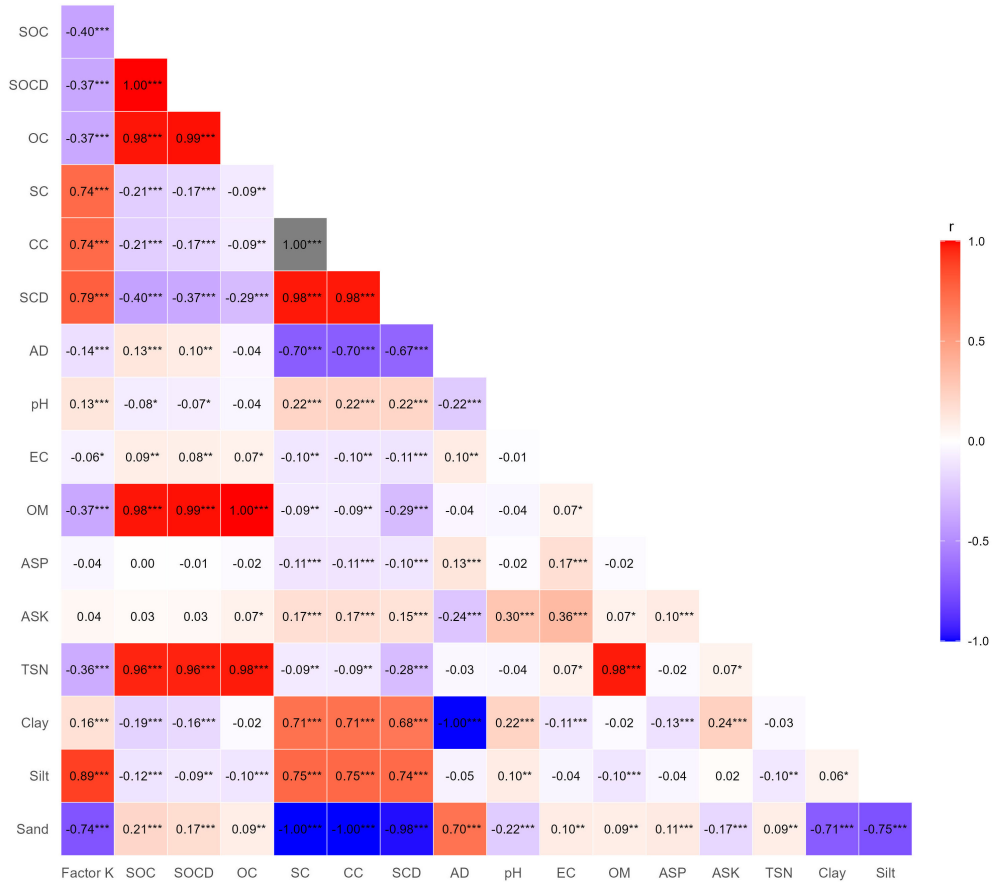

FIGURE 7
Pearson correlation matrix of soil physicochemical and textural properties in the Peruvian Amazon. The color gradient represents the magnitude and direction of correlations (r), and asterisks indicate the levels of statistical significance associated with p-values (* p < 0.05; ** p < 0.01; *** p < 0.001).

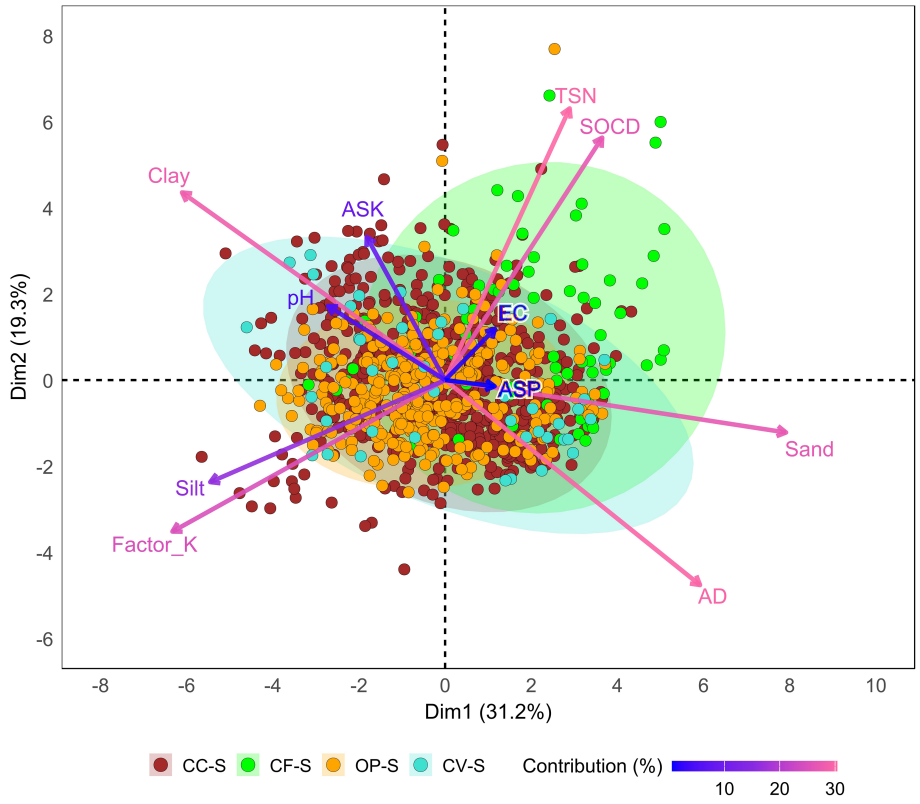

FIGURE 8
Biplot of the principal component analysis (PCA) of soil physical and chemical properties under four canopy structures.

more pronounced variation among systems, with the highest value recorded in the medium density canopy (CC-S: 10.69 ± 3.54 mg kg^{-1}), followed by the intermediate canopy (OP-S: 7.08 ± 2.38 mg kg^{-1}). Inthis sense, the lowest values occurred in the non-canopy (CV-S: 2.66 ± 0.99 mg kg^{-1}) and high density canopy systems (CF-S: 4.34 ± 2.16 mg kg^{-1}) (Figure 4C).

Altogether, a positive trend of TSN associated with increasing canopy cover was evident, with significantly higher values in the CF-S system. This suggests that greater canopy density enhances nitrogen retention and cycling in the soil. Conversely, ASK and ASP did not exhibit a clear trend in relation to canopy cover.

3.3 Soil textural and physicochemical properties

The analysis of variance, complemented by Tukey's *post hoc* test ($p < 0.05$), revealed significant differences in soil textural components and physicochemical properties among systems with contrasting canopy structures (Figure 5, Table 2). Sand content was significantly higher in CF-S (63.2 ± 13.3) compared to the other systems, which did not differ significantly from each other (CC-S: 50.3 ± 13.4%; OP-S: 47.9 ± 12.2%; CV-S: 52.3 ± 17.6%) (Figure 5A). Clay content ranged between 19.2 ± 8.3% and 25.3 ± 9.9%, being significantly lower in CF-S respect to CC-S, OP-S, and CV-S. These systems formed a homogeneous group without statistical differences among them (Figure 5B). Likewise, silt content showed significant differences, with the highest values observed in OP-S (26.8 ± 7.7%) and the lowest in CF-S (17.6 ± 7.2%) (Figure 5C). Systems with dense canopy cover (CF-S and CC-S) exhibited predominantly sandy loam to sandy clay loam textures (SaLo–SaClLo). This result reflects soils more balanced and structurally stable. The intermediate canopy system (OP-S) presented a sandy clay loam texture (SaClLo) marked by good aeration and moderate water retention. In contrast, soils without canopy cover (CV-S) were mainly classified as sandy loam (SaLo), with higher sand content and lower cohesion. These findings indicate greater susceptibility to water erosion (Figure 6). Regarding physicochemical properties, bulk density (AD) differed significantly among systems, with CF-S (1.37 ± 0.11 g cm^{-3}) revealing higher values than the other systems. CC-S (1.30 ± 0.13 g cm^{-3}), CV-S (1.31 ± 0.14 g cm^{-3}) and OP-S (1.30 ± 0.09 g cm^{-3}) did not differ significantly from each other, forming a homogeneous group (Figure 5D). Electrical conductivity (EC) was significantly lower in OP-S (5.2 ± 1.3 mS m^{-1}) and higher in CC-S, CF-S and CV-S (10.1 ± 2.6 to 11.8 ± 3.0 mS m^{-1}), which exhibited similar values (Figure 5E). Soil pH ranged from 4.5 to 5.1, with CF-S (4.49 ± 0.59) being the only system that differed significantly from the others (CC-S: 4.81 ± 0.90; OP-S: 4.97 ± 0.46; CV-S: 5.08 ± 1.10) (Figure 5F).

3.4 Correlation of SOCD and the K factor with soil physicochemical parameters

The Pearson correlation analysis (Figure 6) indicated that the strongest associations of the K factor were linked to the textural fractions, showing a very high positive correlation with silt ($r = 0.89$; $p < 0.001$) and a marked negative correlation with sand ($r = -0.74$;

10.3389/fagro.2026.1769313

TABLE 2 One-way ANOVA was used to evaluate the effect of land-use type, in agroecosystems with different canopy structures, on soil physicochemical and textural properties.

Variable	Source of variation	df	MSE	F	p
K Factor_	Land-use Type	3	0.0549	32.3256	<0.001
	Error	1045	0.0017		
SOCD	Land-use Type	3	29748.2938	46.4779	<0.001
	Error	1045	640.0531		
OC	Land-use Type	3	40.7851	39.0363	<0.001
	Error	1045	1.0448		
SC	Land-use Type	3	633.3225	26.4957	<0.001
	Error	1045	23.9029		
CC	Land-use Type	3	4.7372	26.4957	<0.001
	Error	1045	0.1788		
SCD	Land-use Type	3	967.1059	38.5618	<0.001
	Error	1045	25.0794		
AD	Land-use Type	3	0.1071	7.8134	<0.001
	Error	1045	0.0137		
pH	Land-use Type	3	5.8670	9.7492	<0.001
	Error	1045	0.6018		
EC	Land-use Type	3	2042.9126	42.0073	<0.001
	Error	1045	48.6324		
OM	Land-use Type	3	147.2344	39.0363	<0.001
	Error	1045	3.7717		
ASP	Land-use Type	3	2054.8000	24.4400	<0.001
	Error	1045	84.1000		
ASK	Land-use Type	3	44192.3287	11.6176	<0.001
	Error	1045	3803.9261		
TSN	Land-use Type	3	0.3798	38.4352	<0.001
	Error	1045	0.0099		
Clay	Land-use Type	3	812.3614	10.0926	<0.001
	Error	1045	80.4909		
Silt	Land-use Type	3	1755.9833	19.6956	<0.001
	Error	1045	89.1561		
Sand	Land-use Type	3	4624.8945	26.4794	<0.001
	Error	1045	174.6599		

K Factor, erodibility; SOC, soil organic carbon; SOCD, soil organic carbon density; OC, organic carbon; SC, saturated carbon; CC, critical carbon; SCD, saturated carbon deficit; AD, bulk density; pH, hydrogen potential; EC, electrical conductivity; OM, organic matter; ASP, available soil phosphorus; ASK, available soil potassium; TSN, total soil nitrogen; Sand, Silt, and Clay: textural fractions (%)

$p < 0.001$). A weaker positive correlation was also observed with clay ($r = 0.16$; $p < 0.001$). In contrast, correlations between the K factor and physicochemical properties such as bulk density (BD), pH, electrical conductivity (EC), available soil phosphorus (ASP), and available soil potassium (ASK) were weak, with $|r| < 0.18$. SOCD exhibited its strongest correlation with total soil nitrogen (TSN; $r = 0.96$). Conversely, it displayed weak relationships between the textural fractions (sand, clay, and silt) and the physicochemical variables, all with $|r| < 0.20$.

3.5 Multivariate analysis of soil physical and chemical properties under different canopy structures

The principal component analysis (PCA) illustrated in Figure 8 jointly explained 50.5% of the total variance across two dimensions. Dimension 1 (31.2%) was dominated by Sand and BD, in contrast to the opposite loadings of Clay, Silt, and the K factor. Dimension 2 (19.3%) was primarily driven by SOCD and TSN. The different canopy

structures were associated with distinctive patterns in soil physical and chemical properties. CV-S showed a strong association with Sand, BD, and the K factor, indicating more erodible, sandy, and compact soils under limited vegetation cover. OP-S exhibited a moderate association with pH, ASK, and Silt, reflecting affinity with chemical and textural attributes characteristic of an intermediate canopy. CC-S displayed a moderate-to-strong association with Silt and Clay, suggesting affinity with soils dominated by fine fractions. In contrast, CF-S showed a strong association with SOCD and TSN, indicating correspondence with organic-matter-rich conditions under a dense canopy. The PCA revealed two clearly defined relational patterns. The first corresponded to a strong positive relationship between silt and the K factor, as well as between TSN and SOCD, indicating that silt fractions are associated with greater susceptibility to erosion, whereas soil organic matter and total nitrogen follow a shared gradient of edaphic enrichment. In contrast, a marked negative association was observed between the TSN–SOCD pair and the silt–K factor group, along with the opposition of clay, pH, and ASK against ASP, sand, and bulk density. This pattern reflects opposing edaphic gradients where soils enriched in organic matter and nutrients contrast with those exhibiting higher susceptibility to erosion.

3.6 Spatial variability of soil organic carbon density and soil erodibility estimated by ordinary kriging

The spatial distribution of soil organic carbon density (SOCD) and the erodibility factor (K factor), obtained through ordinary kriging, is presented for four canopy systems located in different districts of the Peruvian Amazon (Figure 9A1–B4): CV-S (cassava, no canopy; Yurimaguas district, A1 and B1), OP-S (oil palm, intermediate canopy; Pólvora district, A2 and B2), CC-S (cacao, medium-density canopy; Soritor district, A3 and B3), and CF-S (coffee, high-density canopy; Rodríguez de Mendoza district, A4 and B4).

The spatial distribution of SOCD showed that the CC-S and CF-S canopy structures exhibited significant spatial autocorrelation, with Moran's I values of 0.30 and 0.49, respectively ($p< 0.05$). These systems also demonstrated the best cross-validation performance between observed and predicted values, with RMSE = 19.18, R^2 = 0.42 for CC-S and RMSE = 19.38, R^2 = 0.48 for CF-S. In contrast, the remaining canopy structures displayed low spatial autocorrelation (Moran's I< 0.2; $p > 0.05$) and low predictive capacity ($R^2< 0.30$), suggesting that their spatial variation is predominantly random and does not exhibit distance-dependent patterns. Regarding the spatial distribution of the K factor, CV-S and CF-S exhibited significant spatial autocorrelation, both with Moran's I values of 0.47 ($p< 0.05$), and recorded the highest cross-validation performance, with RMSE = 0.04, R^2 = 0.48 for CV-S and RMSE = 0.03, R^2 = 0.40 for CF-S. By contrast, the other canopy structures showed low spatial autocorrelation (Moran's I< 0.2; $p > 0.05$) and limited predictive capacity ($R^2< 0.21$), indicating predominantly random spatial variation.

The prediction surfaces of SOCD generated through ordinary kriging showed that the CF-S system (Figure 9A4 exhibited the highest concentrations, with extensive areas ranging from 60

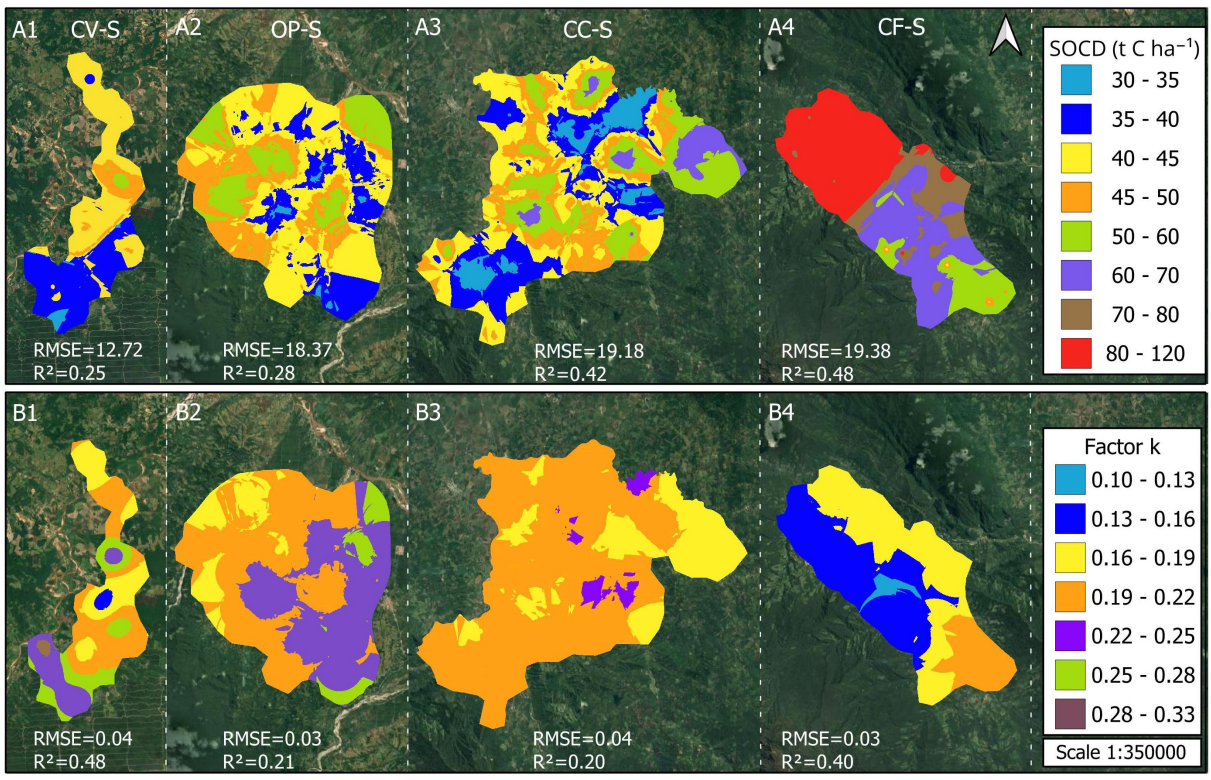

FIGURE 9
Spatial distribution of soil organic carbon density (SOCD) and the soil erodibility factor (Factor K) estimated using ordinary kriging in four agroecosystems with different canopy structures. Panels **(A1–A4)** show SOCD in CV-S, OP-S, CC-S, and CF-S, respectively; panels **(B1–B4)** show the K factor for the same agroecosystems.

to >80 t C ha^{-1}. This was followed by CC-S (Figure 9A3), where intermediate-to-high values (45–65 t C ha^{-1}) predominated. In OP-S (Figure 9A2), moderate levels were observed, mainly between 35–50 t C ha^{-1}, Finally, CV-S (Figure 9A1) recorded the lowest concentrations, dominated by ranges of 31–45 t C ha^{-1}.In general, these values indicate that higher canopy structure is associated with increased SOCD concentrations. With respect to the K factor, the CV-S system (Figure 9B1 showed the highest values, corresponding to high-to-moderate erodibility, with predominant ranges between 0.21–0.32. In OP-S (Figure 9B5), values clustered within the 0.20–0.27 interval, classifying this system as having moderate erodibility. In CC-S (Figure 9B3) ranges between 0.17–0.22 prevailed, reflecting low-to-moderate erodibility. Lastly, CF-S (Figure 9B4) predominantly exhibited the lowest values (≤0.17), placing it within the low-erodibility category according to the USDA reference framework (U.S. Department of Agriculture) (Sharpley and Williams, 1990).

4 Discussions

4.1 Soil organic carbon density and the soil erodibility factor

The results showed a significant increase in SOCD across the four agroecosystems (Figures 2a, b). The coffee-based agroecosystem (CF-S) exhibited the highest SOCD levels. Soil organic carbon density (SOCD) is an important indicator of soil organic carbon (SOC and a key parameter in agricultural soils, providing valuable information for improving environmental quality and agricultural productivity (Liu et al., 2022). The CF-S system showed elevated SOC content, likely due to abundant litterfall and pronounced vegetation stratification, where the decomposition of large amounts of litter contributes substantially to SOC inputs (Cao et al., 2020). Moreover, vegetation roots and soil microorganisms are abundant, and the soil's self-fertilization capacity is high. Increased root exudates and residues accelerate nutrient cycling and improve the efficiency of organic matter formation, promoting SOC accumulation per unit area (Zeng et al., 2023). However, the cassava agroecosystem, being a monoculture, exhibits limited secondary plant cover and reduced litter deposition, resulting in a shallow humus layer in the study area (Lechleitner et al., 2017), This condition led to significant differences compared with the other agroecosystems and contributed to lower SOCD availability (Sokołowska et al., 2020). Moreover, cassava-based ecosystems are temporary systems, and their soils undergo continuous disturbance due to the annual planting cycles. This recurrent soil turnover makes SOCD more vulnerable to external factors (Gaitán et al., 2019; Li et al., 2022), such as climate change, vegetation growth dynamics, environmental shifts, and human activities.

4.2 Soil nutrients under different canopy structures

This study aligns with the findings who observed 0.31% nitrogen in soils from coffee systems associated with shade tree. The higher nitrogen contents in this agroecosystem are likely attributable to the greater organic matter inputs found in the coffee plantations, as documented by Vallejos-Torres et al. (2024). This is translated into increased nitrogen availability. Shade-tree species can influence soil nutritional status both directly (e.g., through litter deposition and nitrogen fixation) and indirectly (e.g., by modifying decomposition rates due to temperature differences beneath the canopy) (Liu et al., 2021; Strukelj et al., 2021). Similarly, total soil nitrogen (N) concentrations in shaded coffee system have been reported to be significantly higher ($P< 0.05$) in the upper soil layer compared with unshaded coffee systems (Xiao et al., 2020). Thus, agroecosystems with shade tres supply biomass to the soil that is decomposed by microfauna, contributing substantially to nitrogen inputs. Regarding available potassium, no significant differences were observed among the coffee, cacao, and cassava agroecosystems. In contrast, available phosphorus was highest in the cacao system. Shade trees are key components of cacao agroforestry systems because they influence yield and soil fertility (Asitoakor et al., 2024). The presence of neighboring shade trees has been shown to increase nitrogen, phosphorus, and pH in the rhizosphere of nearby cacao trees without reducing yield. Over longer time scales, these increases in rhizosphere soil fertility are likely to enhance cacao productivity and shape microbial communities. Theses regression models indicate that nitrogen and phosphorus, in particular, are key predictors of cacao yields and of microbiome diversity and composition (Schmidt et al., 2022).

4.3 Soil textural and physicochemical properties

Egeta et al. (2023) reported an average sand content of 56.93%; and a mean bulk density of 1.49 g cm^{-3} in their forest ecosystem study. These results are comparable to those obtained in the present study, where the coffee agroecosystem exhibited the highest sand content and bulk density. Sand content has been shown to better predict SOC distribution than silt and clay fractions (Saiz et al., 2012). Carbon decomposition is slower in finer-textured soils, contributing to greater chemical stabilization of SOC through adsorption onto soil clay minerals (Krull et al., 2003). Regarding bulk density, the coffee agroecosystem showed the highest values; likely because CF-S represents a permanent and relatively stable agroecosystem over time. This pattern is consistent with findings by Arthur et al. (2022) who reported significantly ($P< 0.05$) lower bulk density in a 23-year-old plantation and higher values in an 18-year-old plantation. In terms of soil pH, the cassava agroecosystem exhibited the highest values, whereas the coffee agroecosystem presented the lowest. These results suggest that both climatic conditions and anthropogenic activities influence the spatial distribution of soil pH (Sun et al., 2023). Moreover, soil pH plays a central role in regulating multiple soil properties. Variations in soil pH may be associated with changes in climate, soil buffering capacity, nitrogen deposition, and vegetation (Hong et al., 2019).

4.4 Correlation of SOCD and the K factor with soil physicochemical parameters

Soil organic carbon (SOC) content results from a net balance between the rate of organic matter input and the rate of organic

carbon mineralization (Sheng et al., 2015), with the former being primarily determined by plant cover and root plant (Zhang et al., 2021). The present study shows a highly significant and positive correlation between total soil nitrogen (TSN) and both SOC and SOCD; that is, as SOC increases, TSN also tends to increase. Because most soil nitrogen is stored in organic matter (Xie et al., 2020), and because increased nitrogen availability enhances microbial activity that promotes decomposition, this process elevates SOC content and its active carbon fraction (Liu et al., 2021; Xu et al., 2020). Likewise, SOC also exhibited a positive correlation with sand (0.21), whereas it showed negative correlations with silt (−0.12) and clay (−0.19). Our findings provide empirical evidence that conservation-oriented agricultural systems such as coffee and cacao agroecosystems enhance and increase the accumulation and persistence of SOC and total soil nitrogen under projected climate-warming scenarios (Tian et al., 2024). Statistical evaluation using Pearson correlation revealed positive correlations between soil erodibility and silt (0.63%), and negative correlations with sand (−0.16%) and organic matter (−0.32%) (Othmani et al., 2023). In addition, Solórzano-Acosta et al. (2025) reported a strong association between SOCD-related properties and organic matter (OM) and total soil nitrogen (TSN) across different vegetation covers.

4.5 Multivariate analysis of soil physicochemical properties under different canopy structures

The PCA confirmed the patterns already observed in the correlation analysis, showing that texture and erodibility constitute the main gradient of edaphic variation, while soil carbon and nitrogen content define a second axis associated with soil fertility. CV-S clustered with sand, bulk density and the K Factor, consistent with its greater erodibility and low carbon content. This result agrees with earlier observation, notably the strong positive relationships between silt, the K factor, and low SOCD values in soils with reduced canopy cover (Gyssels et al., 2005; Sharmeen and Willgoose, 2006; Solórzano-Acosta et al., 2025). In contrast, CF-S was clearly associated with SOCD and TSN, reinforcing the previously described pattern that dense-canopy systems accumulate higher organic matter and nitrogen, in line with the SOCD–TSN coupling identified in the correlation matrix and with findings reported for tropical soils (Cotrufo et al., 2013).

4.6 Spatial distribution of soil organic carbon density and soil erodibility based on ordinary kriging

The spatial analysis using ordinary kriging showed that canopy structure clearly influences the distribution of soil organic carbon density (SOCD) and erodibility (K factor). Agroecosystems with denser canopies, particularly CF-S and CC-S, exhibited the highest SOCD concentrations, with averages of 82.64 t C ha^{-1} and 60.66 t C ha^{-1}, respectively. This pattern is in line with studies indicating that well-developed vegetation cover enhances soil carbon accumulation due to increased residue inputs and greater surface stability provided by vegetation (Vallejos-Torres et al., 2024). Additionally, the contribution of roots and stable aggregates—widely recognized as mechanisms promoting carbon retention in tropical soils—further supports this pattern (Mustafa et al., 2020; Srivastava and Yetgin, 2024). Conversely, agroecosystems with reduced canopy cover, such as OP-S and CV-S, recorded the lowest SOCD values, with averages of 46.59 t C ha^{-1} and 32.68 t C ha^{-1}, respectively. In humid forests, strong biomass recovery and growth largely compensated for carbon losses caused by deforestation and degradation; moreover, as observed in African forests and woody savannas, these ecosystems have historically acted as carbon sinks by removing atmospheric carbon and storing it as biomass (Zhao et al., 2024; Rodríguez-Veiga et al., 2025). Regarding the K factor, the highest values were concentrated in CV-S (0.21–0.32), confirming that low-cover soils are more susceptible to erosion. OP-S exhibited moderate erodibility (0.20–0.27), whereas CC-S presented lower values (0.17–0.22). The lowest erodibility was observed in CF-S (≤ 0.17), indicating reduced vulnerability to detachment.

From a methodological perspective, the variable performance of the geostatistical models employed should be acknowledged as a limitation. Although ordinary kriging allowed the identification of general spatial trends, semivariogram analyses revealed low spatial autocorrelation of soil organic carbon density and the soil erodibility factor across the evaluated agroecosystems, indicating that values are randomly distributed in space and exhibit a spatial pattern compatible with randomness. This condition limits the ability of the model to generate robust local estimates and indicates that, at the sampling scale considered, no sufficiently well-defined spatial structure is detected to support high-precision point predictions.

5 Conclusions

Along the evaluated gradient, agroecosystems with greater tree canopy cover exhibited a substantially higher accumulation of soil organic carbon. This response indicates that dense agroecosystems enhance biomass inputs, maintain more stable microclimates, and promote organic matter stabilization processes. Consequently, they consolidate their role as remarkable components for carbon storage in Amazonian agricultural landscapes. In a complementary manner, the erodibility factor (K) showed an inverse pattern, consistently decreasing from 0.31 in CV-S to 0.16 in CF-S. The combined behavior of SOCD and the K factor reveals a functional gradient in which canopy development simultaneously enhances soil fertility and resistance to erosive processes. On the other hand, soil erodibility was mainly driven by texture, as evidenced by its strong positive correlation with silt (r = 0.89) and negative correlation with sand (r = −0.74). This demonstrates that fine fractions favor soil disaggregation under conditions of limited vegetation cover. Multivariate analyses corroborated these trends, showing that agroecosystems without canopy cover are associated with higher erodibility, greater bulk density, and sandier textures,

whereas dense canopy systems cluster with elevated SOCD and TSN values, representing soils that are more fertile, stable, and resilient. Taken together, these findings highlight that canopy-covered agroecosystems act as a central ecological regulator in the Peruvian Amazon; therefore, integrating agricultural crops with dense tree cover emerges as an effective strategy to enhance carbon sequestration, reduce soil erodibility, and improve soil stability and sustainability, thereby contributing to the resilient management of Amazonian agricultural landscapes.

Data availability statement

The raw data supporting the conclusions of this article will be made available by the authors, without undue reservation.

Author contributions

RC-R: Investigation, Supervision, Methodology, Writing – review & editing, Resources. RS: Project administration, Funding acquisition, Data curation, Writing – original draft, Formal analysis. JC: Funding acquisition, Writing – original draft, Conceptualization, Formal analysis, Data curation. GV-T: Visualization, Validation, Writing – original draft, Methodology, Investigation.

Funding

The author(s) declared that financial support was received for this work and/or its publication. The research was funded by the Instituto Nacional de Innovación Agraria, within the framework of the project: Mejoramiento de los servicios de investigación y transferencia tecnológica en el manejo y recuperación de suelos agrícolas degradados y aguas para riego en la pequeña y mediana agricultura en los departamentos de Lima, Áncash, San Martín, Cajamarca, Lambayeque, Junín, Ayacucho, Arequipa, Puno y Ucayali" CUI 2487112.

Conflict of interest

The author(s) declared that this work was conducted in the absence of any commercial or financial relationships that could be construed as a potential conflict of interest.

Generative AI statement

The author(s) declared that generative AI was not used in the creation of this manuscript.

Any alternative text (alt text) provided alongside figures in this article has been generated by Frontiers with the support of artificial intelligence and reasonable efforts have been made to ensure accuracy, including review by the authors wherever possible. If you identify any issues, please contact us.

Publisher's note

References

Arthur, A., Acquaye, S., Cheng, W., Dogbatse, J. A., Konlan, S., Domfeh, O., et al. (2022). Soil carbon stocks and main nutrients under cocoa plantations of different ages. *Soil Sci. Plant Nutr.* 68, 99–103. doi: 10.1080/00380768.2022.2029219

Asitoakor, B. K., Anders Ræbild, A., Vaast, P., Ravn, H. P., Owusu, K., Mensah, E. O., et al. (2024). "Shade Trees Species Matter: Sustainable Cocoa-Agroforestry Management," in *Agroforestry as Climate Change Adaptation*. Eds. M. F. Olwig, A. Skovmand Bosselmann and K. Owusu (Palgrave Macmillan, Cham). doi: 10.1007/978-3-031-45635-0_3

Batjes, N. H. (1996). Total carbon and nitrogen in the soils of the world. *Eur. J. Soil Sci.* 47, 151–163. doi: 10.1111/j.1365-2389.1996.tb01386.x

Bremner, J. M. (1996). Nitrogen-total. *Methods Soil analysis: Part 3 Chem. Methods* 5, 1085–1121. doi: 10.2136/sssabookser5.3.c37

Cao, J., He, X., Chen, Y., Chen, Y., Zhang, Y., Yu, S., et al. (2020). Leaf litter contributes more to soil organic carbon than fine roots in two 10-year-old subtropical plantations. *Sci. Total Environ.* 704, 135341. doi: 10.1016/j.scitotenv.2019.135341

Castellano-Hinojosa, A., and Strauss, S. L. (2020). Impact of cover crops on the soil microbiome of tree crops. *Microorganisms* 8, 328. doi: 10.3390/microorganisms8030328

Cerda, R., Avelino, J., Harvey, C. A., Gary, Ch., Tixier, P., Allinne, C., et al. (2020). Coffee agroforestry systems capable of reducing disease-induced yield and economic losses while providing multiple ecosystem services. *Crop Prot* 134, 105149. doi: 10.1016/j.cropro.2020.105149

Cotrufo, M. F., Wallenstein, M. D., Boot, C. M., Denef, K., and Paul, E. (2013). The Microbial Efficiency-Matrix Stabilization (MEMS) framework integrates plant litter decomposition with soil organic matter stabilization: do labile plant inputs form stable soil organic matter? *Global Change Biol.* 19, 988–995. doi: 10.1111/gcb.12113

Coulibaly, K. (2024). Geostatistical modelling of physico-chemical properties of soils. *Int. J. Geo-Information Sci.* 13, 221–235. doi: 10.1080/27658511.2024.233363

De Corato, U., Viola, E., Keswani, C., and Minkina, T. (2024). Impact of the sustainable agricultural practices for governing soil health from the perspective of a rising agri-based circular bioeconomy. *Appl. Soil Ecol.* 194, 105199. doi: 10.1016/j.apsoil.2023.105199

Egeta, D., Negash, M., Alebachew, M., Eshete, A., Mulugeta, S., and Lemi, T. (2023). Species-specific allometric equations, biomass expansion factor, and wood density of native tree species in the dry afromontane forest of Ethiopia. *Int. J. Forestry Res.* 2023, 5572048. doi: 10.1155/2023/5572048

European Space Agency (ESA) (2021). *Copernicus digital elevation model (DEM) – GLO-30 [Data set]* (Copernicus Programme: European Space Agency (ESA) y Airbus). doi: 10.5270/ESA-c5d3d65

Gaitán, J. J., Maestre, F. T., Bran, D. E., Buono, G. G., Dougill, A. J., García, G., et al. (2019). Biotic and abiotic drivers of topsoil organic carbon concentration in drylands have similar effects at regional and global scales. *Ecosystems* 22, 1445–1456. doi: 10.1007/s10021-019-00348-y

Gyssels, G., Poesen, J., Bochet, E., and Li, Y. (2005). Impact of plant roots on the resistance of soils to erosion by water: A review. *Prog. Phys. Geogr.* 29, 189–217. doi: 10.1191/0309133305pp443ra

Hao, X. X., Han, X. Z., Li, L. J., Zou, W. X., Lu, X. C., and Qiao, Y. F. (2015). Profile distribution and storage of soil organic carbon in a black soil as affected by land use types. *Ying Yong Sheng Tai Xue* 26, 965–972. Available online at: https://pubmed.ncbi.nlm.nih.gov/26259435/ (Accessed October 17, 2025).

Hong, S., Gan, P., and Chen, A. (2019). Environmental controls on soil pH in planted forest and its response to nitrogen deposition. *Environ. Res.* 172, 159–165. doi: 10.1016/j.envres.2019.02.020

INRENA (1996). *Mapa de suelos del Perú* (Lima, Peru: Instituto Nacional de Recursos Naturales). Available online at: https://alicia.concytec.gob.pe/vufind/Record/ANAI_28747f8eca9c40b0012ef93baa9cbfcb (Accessed November 01, 2025).

Krull, E. S., Baldock, J. A., and Skjemstad, J. O. (2003). Importance of mechanisms and processes of the stabilisation of soil organic matter for modelling carbon turnover. *Funct. Plant Biol.* 30, 207–222. doi: 10.1071/FP02085

Lechleitner, F. A., Dittmar, T., Baldini, J. U., Prufer, K. M., and Eglinton, T. I. (2017). Molecular signatures of dissolved organic matter in a tropical karst system. *Organic Geochem.* 113, 141–149. doi: 10.1016/j.orggeochem.2017.07.015

Li, Y. G., Liu, W., Feng, Q., Zhu, M., Yang, L. S., and Zhang, J. T. (2022). Effects of land use and land cover change on soil organic carbon storage in the hexi regions, Northwest China. *J. Environ. Manage.* 312, 114911. doi: 10.1016/j.jenvman.2022.114911

Liu, Q., He, L., Guo, L., Wang, M., Deng, D., Lv, P., et al. (2022). Digital mapping of soil organic carbon density using newly developed bare soil spectral indices and deep neural network. *Catena (Amst)* 219, 106603. doi: 10.1016/j.catena.2022.106603

Liu, M., Li, P., Liu, M., Wang, J., and Chang, Q. (2021). The trend of soil organic carbon fractions related to the successions of different vegetation types on the tableland of the Loess Plateau of China. *J. Soils Sediments* 21, 203–214. doi: 10.1007/s11368-020-02710-3

Liu, P., Wang, W., Bai, Z., Guo, Z., Ren, W., Huang, J., et al. (2021). Nutrient loads and ratios both explain the coexistence of dominant tree species in a boreal forest in Xinjiang, Northwest China. *For. Ecol. Manage.* 491, 119198. doi: 10.1016/j.foreco.2021.119198

Mustafa, A., Minggang, X., Shah, S. A. A., Abrar, M. M., Nan, S., Baoren, W., et al. (2020). Soil aggregation and soil aggregate stability regulate organic carbon and nitrogen storage in a red soil of southern China. *J. Environ. Manage.* 270, 110894. doi: 10.1016/j.jenvman.2020.110894

NOM-021-RECNAT-2000 (2002). Natural resources and environment secretary. Mexican official standard. Specifications of fertility, salinity, and soil classification. Study, sampling and analysis. Available online at: https://www.ordenjuridico.gob.mx/Documentos/Federal/wo69255.pdf (Accessed November 11, 2025)

Olsen, S. R., and Sommers, L. E. (1982). "Phosphorus," in *Methods of Soil Analysis Part 2 Chemical and Microbiological Properties*. Ed. A. L. Page (American Society of Agronomy, Soil Science Society of America, Madison), 403–430. doi: 10.2134/agronmonogr9.2.2ed.c24

Orton, T., Pringle, M. J., Page, K. L., Dalal, R. C., and Bishop, T. F. (2014). Spatial prediction of soil organic carbon stock using a linear model of coregionalisation. *Geoderma* 230, 119–130. doi: 10.1016/j.geoderma.2014.04.016

Othmani, O., Khanchoul, K., Boubehziz, S., Bouguerra, H., Benslama, A., and Navarro-Pedreño, J. (2023). Spatial Variability of Soil Erodibility at the Rhirane Catchment Using Geostatistical Analysis. *Soil Systems* 7, 32. doi: 10.3390/soilsystems7020032

Pereira, G. W., and Valente, R. A. (2022). Smart-Map: An open-source QGIS plugin for digital soil mapping. *Agronomy* 12, 1350. doi: 10.3390/agronomy12061350

Posit Team (2025). *RStudio: Integrated development environment for R* (Boston, MA, United States: Posit Software, PBC).

QGIS Development Team (2024). QGIS geographic information system (Version 3.34.14 prizren) (Open Source Geospatial Foundation: QGIS.ORG Association). Available online at: https://qgis.org.

R Core Team (2025). *R: A language and environment for statistical computing* (R Foundation for Statistical Computing). Available online at: https://www.r-project.org/ (Accessed October 21, 2025).

Rodríguez-Veiga, P., Carreiras, J. M. B., Quegan, S., Heiskanen, J., Pellikka, P., Adhikari, H., et al. (2025). Loss of tropical moist broadleaf forest has turned Africa's forests from a carbon sink into a source. *Sci. Rep.* 15, 41744. doi: 10.1038/s41598-025-27462-3

Rolo, V., Rivest, D., Maillard, É., and Moreno, G. (2023). Agroforestry potential for adaptation to climate change: A soil-based perspective. *Soil Use Manage.* 39, 1006–1032. doi: 10.1111/sum.12932

Saiz, G., Bird, M. I., Domingues, T., Schrodt, F., Schwarz, M., Feldpausch, T. R., et al. (2012). Variation in soil carbon stocks and their determinants across a precipitation gradient in West A frica. *Global Change Biol.* 18, 1670–1683. doi: 10.1111/j.1365-2486.2012.02657.x

Schmidt, J. E., Firl, A., Hamran, H., Imaniar, N. I., Crow, T. M., and Forbes, S. J. (2022). Impacts of shade trees on the adjacent cacao rhizosphere in a young diversified agroforestry system. *Agronomy* 12, 195. doi: 10.3390/agronomy12010195

SENAMHI (2014). *Boletín climático de la región San Martín* (Servicio Nacional de Meteorología e Hidrología del Perú). Available online at: https://repositorio.senamhi.gob.pe/handle/20.500.12542/3940 (Accessed November 18, 2025).

SERNANP – Servicio Nacional de Áreas Naturales Protegidas por el Estado (2017). *Diagnóstico biofisico de los bosques montanos del nororiente Peruano* (Lima: SERNANP). Available online at: https://www.gob.pe/sernanp (Accessed October 17, 2025).

Sharmeen, S., and Willgoose, G. (2006). Characteristics of overland flow resistance on bare soil surfaces. *Water Resour. Res.* 42, W05415. doi: 10.1029/2005WR004271

Sharpley, A. N., and Williams, J. R. (1990). EPIC Erosion/Productivity Impact Calculator: 1. Model Documentation. *USA Department of Agriculture Technical Bulletin No. 1768.* (Washington DC: USA Government Printing Office). Available online at: https://www.scirp.org/reference/referencespapers?referenceid=1307268 (Accessed October 02, 2025).

Sheng, H., Zhou, P., Zhang, Y., Kuzyakov, Y., Zhou, Q., Ge, T., et al. (2015). Loss of labile organic carbon from subsoil due to land-use changes in sub-tropical China. *Soil Biol. Biochem.* 88, 148–157. doi: 10.1016/j.soilbio.2015.05.015

Sokołowska, J., Józefowska, A., Woźnica, K., and Zaleski, T. (2020). Succession from meadow to mature forest: Impacts on soil biological, chemical and physical properties—Evidence from the Pieniny Mountains, Poland. *Catena* 189, 104503. doi: 10.1016/j.catena.2020.104503

Solórzano-Acosta, R., Cruz-Luis, J., Chuchon-Remon, R., Romero-Chávez, L. E., Lozano, A., Gaona-Jimenez, N., et al. (2025). The conversion of forests to agricultural croplands significantly depletes soil organic carbon reserves, total nitrogen, and available potassium, reaching critical thresholds in the Peruvian Amazon. *Front. Soil Sci.* 5. doi: 10.3389/fsoil.2025.1662180

Srivastava, R. K., and Yetgin, A. (2024). An overall review on influence of root architecture on soil carbon sequestration potential. *Theor. Exp. Plant Physiol.* 36, 165–178. doi: 10.1007/s40626-024-00323-6

Strukelj, M., Parker, W., Corcket, E., Augusto, L., Khlifa, R., Jactel, H., et al. (2021). Tree species richness and water availability interact to affect soil microbial processes. *Soil Biol. Biochem.* 155, 108180. doi: 10.1016/j.soilbio.2021.108180

Sun, W., Li, S., Zhang, G., Fu, G., Qi, H., and Li, T. (2023). Effects of climate change and anthropogenic activities on soil pH in grassland regions on the Tibetan Plateau. *Global Ecol. Conserv.* 45, e02532. doi: 10.1016/j.gecco.2023.e02532

Tian, J., Dungait, J. A. J., Hou, R., Deng, Y., Hartley, I. P., Yang, Y., et al. (2024). Microbially mediated mechanisms underlie soil carbon accrual by conservation agriculture under decade-long warming. *Nat. Commun.* 15, 377. doi: 10.1038/s41467-023-44647-4

Vallejos-Torres, G., Gaona-Jimenez, N., Lozano, A., Paredes Ch., I., Lozano, C. M., Alva-Arévalo, A., et al. (2023a). Soil organic carbon balance across contrasting plant cover ecosystems in the Peruvian Amazon. *Chilean J. Agric. Res.* 83, 553–564. doi: 10.4067/s0718-58392023000500553

Vallejos-Torres, G., Gaona-Jimenez, N., Ordoñez-Sánchez, L., Lozano, C., Arevalo Alva, A., Lozano, A., et al. (2023b). Effects of arbuscular mycorrhizal fungi, poultry manure compost, and cadmium on plant growth and nutrient absorption of *Oryza sativa*. *Chilean J. Agric. Res.* 83, 656–665. doi: 10.4067/S0718-58392023000600656

Vallejos-Torres, G., Gaona-Jimenez, N., Pichis-García, R., Ordoñez, L., García-Gonzales, P., Quinteros, A., et al (2024). Carbon reserves in coffee agroforestry in the Peruvian Amazon. *Front. Plant Sci.* 15, 1410418. doi: 10.3389/fpls.2024.1410418

Williams, J. R., Jones, C. A., and Dyke, P. T. (1984). A modeling approach to determining the relationship between erosion and soil productivity. *Trans. Asae* 27, 129–144. Available online at: https://elibrary.asabe.org/abstract.asp?aid=32748 (Accessed December 18, 2025).

Xiao, Z., Bai, X., Zhao, M., Luo, K., Zhou, H., Ma, G., et al. (2020). Soil organic carbon storage by shaded and unshaded coffee systems and its implications for climate change mitigation in China. *J. Agric. Sci.* 158, 687–694. doi: 10.1017/S002185962100006X

Xie, B., Zhang, C., and Xie, Y. (2020). Global convergence in correlations among soil properties. *Int. J. Agric. Biol. Engineering* 13, 108–116. doi: 10.25165/10.25165/j.ijabe.20201303.4547

Xu, H. Q., Qing, L., Bing, B. Z., Yue, L., and Guo, B. X. (2020). Variation in soil organic carbon stability and driving factors after vegetation restoration in different vegetation zones on the Loess Plateau, China. *Soil Tillage Res.* 204, 104727. doi: 10.1016/j.still.2020.104727

Zarychta, R. (2025). Application of geostatistical approach in generating digital elevation models from UAV-SfM data. *Geomorphology* 465, 110720. doi: 10.1016/j.geomorph.2025.110720

Zeng, C., Li, T., He, B., Feng, M., and Liang, K. (2023). Effects of vegetation succession on topsoil C, N, and P contents and stoichiometry following agricultural abandonment in a representative karst trough valley. *Ecol. Eng.* 192, 106989. doi: 10.1016/j.ecoleng.2023.106989

Zhang, Y., Ai, J., Sun, Q., Li, Z., Hou, L., Song, L., et al. (2021). Soil organic carbon and total nitrogen stocks as affected by vegetation types and altitude across the mountainous regions in the Yunnan Province, south-western China. *Catena* 196, 104872. doi: 10.1016/j.catena.2020.104872

Zhao, Z., Ciais, P., Wigneron, J. P., Santoro, M., Brandt, M., Kleinschroth, F., et al. (2024). Central African biomass carbon losses and gains during 2010–2019. *One Earth* 7, 506–519. doi: 10.1016/j.oneear.2024.01.021

Zhao, J., Feng, X., Deng, L., Yang, Y., Zhao, Z., Zhao, P., et al. (2020). Quantifying the effects of vegetation restorations on the soil erosion export and nutrient loss on the loess plateau. *Front. Plant Sci.* 11. doi: 10.3389/fpls.2020.573126

Zhu, X., Liu, W., Chen, J., Bruijnzeel, L. A., Mao, Z., Yang, X., et al. (2020). Reductions in water, soil and nutrient losses and pesticide pollution in agroforestry practices: a review of evidence and processes. *Plant Soil* 453, 45–86. doi: 10.1007/s11104-019-04377-3